COMPOSITIONAL MODIFICATION OF ALLOY 706

Tatsuya Takahashi*, Takashi Shibata*, Junichi Taira**, Terutaka Kure**

Muroran Reserch Laboratory*, Muroran Plant**

The Japan Steel Works, LTD.

4 Chatsu-machi, Muroran, Hokkaido 051-8505, Japan

Abstract

Ni-Fe base superalloy 706 has been used for land based turbines. In this study, in order to improve its mechanical properties and producibility, compositional modification was conducted. The strength increases and the ductility decreases, with increasing titanium and niobium content. However, segregation is promoted by the increased niobium. The 0.2% yield strength decreases, although the tensile strength and the ductility does not change, with increasing aluminum. The intragranular precipitation behavior is greatly affected by the contents of the strengthening elements. In order for γ'-γ'' co-precipitates to appear, these three strengthening elements, titanium, niobium and aluminum, must simultaneously exit, and their contents are limited within certain ranges. As a result, a newly modified composition was presented. Then, a large-size trial disk with this modified composition was manufactured from a VIM-ESR ingot. Investigation of the trial disk confirms that it has good mechanical properies without any segregation.

Superalloys 718, 625, 706 and Various Derivatives

Edited by E.A. Loria

TMS (The Minerals, Metals & Materials Society), 2001

Introduction

The tendency towards power generating plants with higher efficiency becomes more and more apparent for reasons of energy problem backed by the global environmental issues. The ultra-super critical pressure or gas turbine power generating plants, therefore, tend to require a higher operating temperature, and the turbine entrance temperature has currently reached even 1500°C.

In the large-scale gas turbines for the combined cycle power generation, Ni-Fe base superalloys 706 and 718 have already been used for a turbine disk material[1-3]. The alloys are known to be age-hardened by the precipitation of coherent γ', γ'' and/or γ' - γ'' co-precipitates in the austenitic matrix[4,5]. However, macro segregation is easily generated in large ingots, because Alloy 706 and Alloy 718 contain a large amount of Al, Ti, and Nb as precipitation strengthening elements. Therefore, even if a special melting method such as electroslag remelting (ESR) or vacuum arc remelting (VAR) is employed, it is difficult to manufacture a large-scale ingot without the segregation. Alloy 718 is inferior to Alloy 706 in producibility, specifically in ingot making and hot working. On the other hand, Alloy 706 is inferior to Alloy 718 in strength. Then, we have developed a new Ni based superalloy for a next generation gas turbine generator material, which has almost the same strength as that of Alloy718 and more excellent producibility than that of Alloy706.

Only Ti and Nb play an important role in precipitation strengthening of Alloys 706 and 718, while Al and Ta are also known as precipitation strengthening elements, in general. In Alloy 706 and Alloy 718, it has been reported that Ti and Nb can be substituted for the Al site of γ' phase[4,6] and Ta can be substituted for the Nb site of γ'' phase[7,8]. Accordingly, it is an important investigation item to clarify the effect of these elements on strengthening for the material development. In this study, in order to improve its mechanical properties and producibility, compositional modification was conducted.

Procedure

Materials

thirteen heats of experimental 50 kg ingot were melted by vacuum induction melting (VIM) furnace. The chemical composition of each heat is listed in Table I. Alloy 706 was within the specification of AMS 5702. Contents of strengthening elements, Al, Ti, Nb, and Ta were systematically varied. As shown in Table I, contents of Ti and Al in experimental alloys Nos. 1 through 10 ranged from 1.0 to 3.1wt.% and from 0.3 to 0.5wt.%, respectively with different content of Nb. The sum of Nb and Ta content in Nos. 11 and 12 was adjusted to 1.0at.% and 2.0at.% with, respectively the same proportion of Ta substitution ratio (Ta / (Nb+Ta)).

All the ingots were diffusion treated and subsequently forged to the billets with a cross section of $30^{t} \times 120^{w}$ mm^2. The billets were sectioned mechanically into samples of suitable sizes. The condition of solution treatment for each heat was determined from the results of hardness measurement and structure observation by optical microscopy. Temperatures of solution treatment for Alloy 706 and experimental Alloys Nos. 1, 2, 4, and 5 was 980°C. Those for alloys Nos. 7 through 10 and Nos. 3, 6, 11, and 12 were 1020°C and 1040°C, respectively. After the solution heat treatment, the samples were cooled down to room temperature with the same cooling rate, 10°C/min. Subsequently they were double-aged at 720°C for 8h and at 620°C for 8h, followed by furnace cooling.

Table I Chemical Composition of Experimental Alloys

(wt.%)

	C	Si	Mn	P	S	Ni	Fe	Cr	Al	Ti	Nb	Ta	Remarks
706	0.004	0.01	0.01	<0.003	0.0009	41.72	37.00	16.43	0.28	1.65	2.89	-	
No. 1	0.004	0.01	0.01	<0.003	0.0011	43.21	37.24	16.59	0.28	**1.69**	**0.97**	-	*1
No. 2	0.006	0.01	0.01	<0.003	0.0012	43.21	36.94	16.48	0.27	**2.07**	**1.00**	-	*1
No. 3	0.006	0.01	0.01	<0.003	0.0017	43.50	35.80	16.29	0.26	**3.11**	**1.01**	-	*1
No. 4	0.005	0.01	0.01	<0.003	0.0012	43.11	36.91	16.68	0.30	**1.00**	**1.96**	-	*2
No. 5	0.007	0.01	0.01	<0.003	0.0011	43.35	36.01	16.57	0.29	**1.72**	**2.03**	-	*2
No. 6	0.004	0.01	0.01	<0.003	0.0013	43.48	34.50	16.66	0.28	**3.03**	**2.02**	-	*2
No. 7	<.003	0.01	0.01	<.003	0.0017	42.70	35.56	16.05	**0.52**	2.52	**2.07**	-	*3
No. 8	0.003	0.01	0.01	<.003	0.0009	42.75	35.2	16.02	**0.77**	2.55	**2.10**	-	*3
No. 9	<.003	0.01	0.01	<.003	0.0009	42.80	35.18	15.98	**0.29**	2.50	**2.56**	-	*4
No. 10	<.003	0.01	0.01	<.003	0.0006	42.74	34.9	15.98	**0.52**	2.52	**2.55**	**0.01**	*4, *7
No. 11	<.003	0.01	0.01	<.003	0.0007	42.84	35.49	16.05	0.50	2.51	**0.78**	**1.61**	*5
No. 12	<.003	0.01	0.01	<.003	0.0008	42.81	34.35	16.00	0.50	2.48	**1.17**	**2.36**	*6

*1 Nb : 1.0wt.% (varied Ti content)
*2 Nb : 2.0wt.% (varied Ti content)
*3 Nb : 2.0wt.% (varied Al content)
*4 Nb : 2.5wt.% (varied Al content)
*5 Ta+Nb=1.0at.%, Ta / (Nb+Ta)=0.50
*6 Ta+Nb=1.5at.%, Ta / (Nb+Ta)=0.51
*7 Ta+Nb=1.5at.%, Ta / (Nb+Ta)=0

Evaluation of Mechanical Properties and Precipitation Behavior

Tensile tests were performed at room temperature, on the double-aged samples. The diameter of specimens was 7mm and the gauge length was 35mm. The double-aged samples were etched with 50% aqua regina ethanol solution after polishing, and the precipitation behavior was observed by scanning electron microscopy (SEM). In addition, the thin samples made by electropolishing with 10% sulfuric acid ethanol solution or 5% perchloric acid acetic acid solution were investigated by transmission electron microscopy (TEM). A 200kV TEM was used with micro-beam techniques in both electron diffraction and energy dispersive X-ray spectroscopy (EDS), with the probe diameter being 0.5 - 5nm.

Results and Discussion

Effect of Ti Content

The variation of tensile properties with Ti content of alloys Nos. 1-3 and alloys Nos. 4-6 are shown in Figure 1. For both 1.0wt.% Nb base alloys and 2.0wt.% Nb base alloys, tensile strength and 0.2% yield strength increased, whereas elongation and reduction of area decreased greatly, with increasing Ti content.

In order to clarify the reason for the degrading in tensile ductility, the grain boundary structure was observed by SEM as seen in Figure 2. In case of low Ti content, no precipitate was observed at grain boundaries regardless of the Nb content, (a), (b), (d), (e). The cellular precipitates were observed in 3.0wt.% Ti alloys, (c), (f). The amount of precipitates was larger in high Nb alloys than low Nb alloys.

These cellular precipitates at grain boundaries were identified as η phase by micro-beam diffraction and EDS. It is reported[9] that only the η phase is the grain boundary precipitate in Alloy 706, and that the moderate existence of η phase at grain boundaries remarkably improves creep strength, although the ductility and toughness is decreased. In fact, Figure 1 indicates that the elongation and the reduction of area rapidly decreased, in accordance with the occurrence of η phase.

TEM images and selected area diffraction patterns of the inside of grains of alloys Nos. 1-3 are shown in Figure 3. The spherical precipitates were clearly observed in the grain interior. These spherical precipitates were identified as γ' phase having FCC structure by micro-beam electron diffraction and EDS. Alloys Nos. 1-3 are hardened by γ' phase regardless of the Ti content. The size of γ' phase in alloy No. 1 (a) and Alloy No. 2 (b) were approximately 20nm, while that of coarse γ' phase observed in alloy No. 3 (c) was about 50nm.

Figure 4 shows TEM images and selected area diffraction patterns of the inside of grains of alloys Nos. 4-6. In contrast to alloys Nos. 1-3, it was confirmed that the intragranular precipitates had

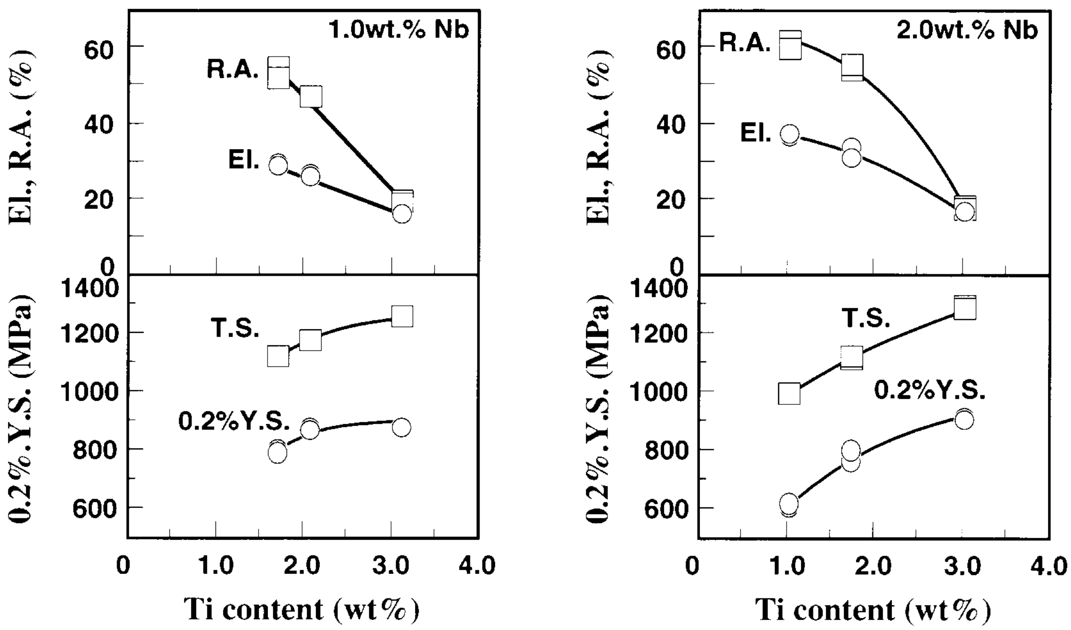

Figure 1: Variation of the tensile properties at room temperature with Ti content.

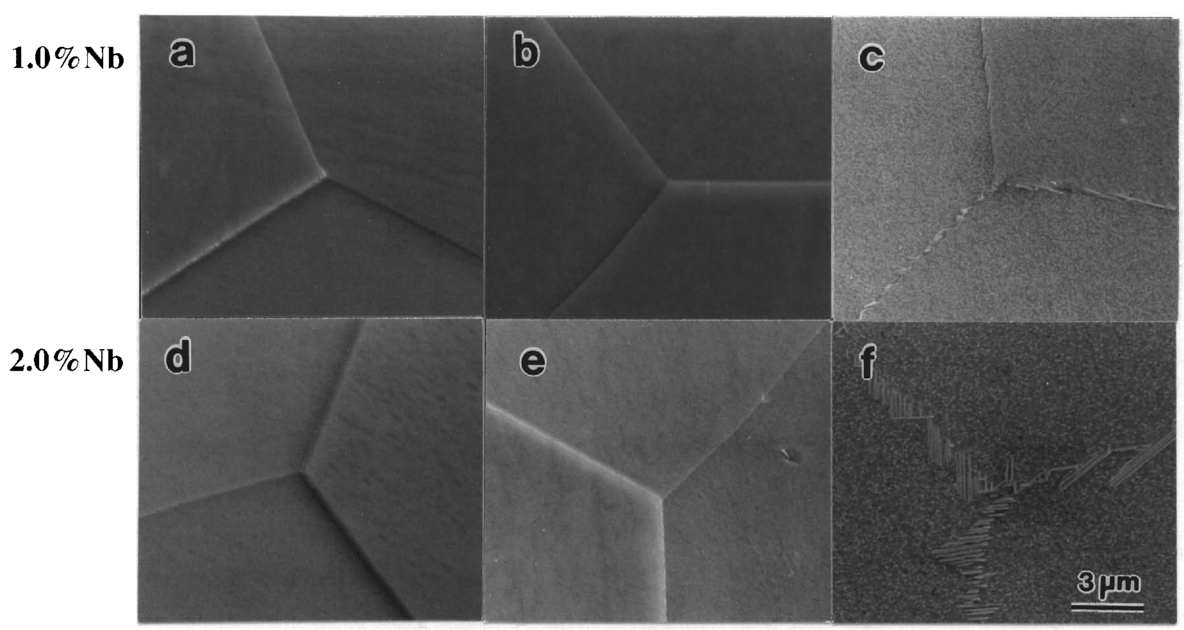

Figure 2: Typical SEM micrographs of grain boudary microstructure, alloys (a) No. 1, (b) No. 2, (c) No. 3, (d) No. 4, (e) No. 5, and (f) No. 6.

changed with increasing Ti content from γ' phase in alloy No. 4 (a) to γ'-γ'' co precipitates in alloys Nos. 5 (b) and 6 (c). Double cuboidal and overlaid γ'-γ'' co-precipitates known as "compact morphology" and "non-compact morphology"[6,10-12], simultaneously existed in alloy No. 6 (c), although only double cuboidal γ'-γ'' co-precipitates were existed in alloy No. 5 (b). These precipitates were the same kinds as the intragranular precipitates appeared in Alloy 706 or modified 718[6,10-12]. As well as the coarse double cuboidal γ'-γ'' and moreover, the fine overlaid γ'-γ'' co-precipitates existed inside the grain of alloy No. 6.

<u>Effect of Nb content</u>

The variation of tensile properties with Nb content of alloys Nos. 1 and 5, Alloy 706, and alloys Nos. 3 and 6 are shown in Figure 5. For both 1.7wt.% Ti base alloys and 3.0wt.% Ti base alloys, tensile strength and 0.2% yield strength increased, whereas elongation and reduction of area decreased, with increasing Nb content. However, decrease in ductility was much small compared with the increase in strength.

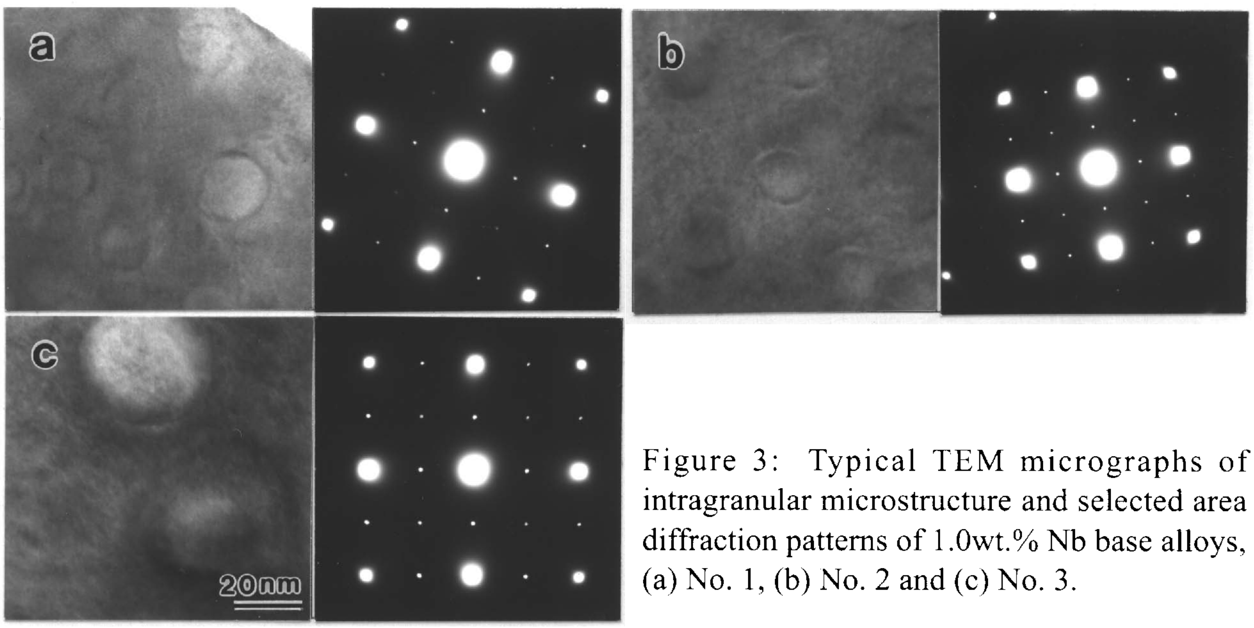

Figure 3: Typical TEM micrographs of intragranular microstructure and selected area diffraction patterns of 1.0wt.% Nb base alloys, (a) No. 1, (b) No. 2 and (c) No. 3.

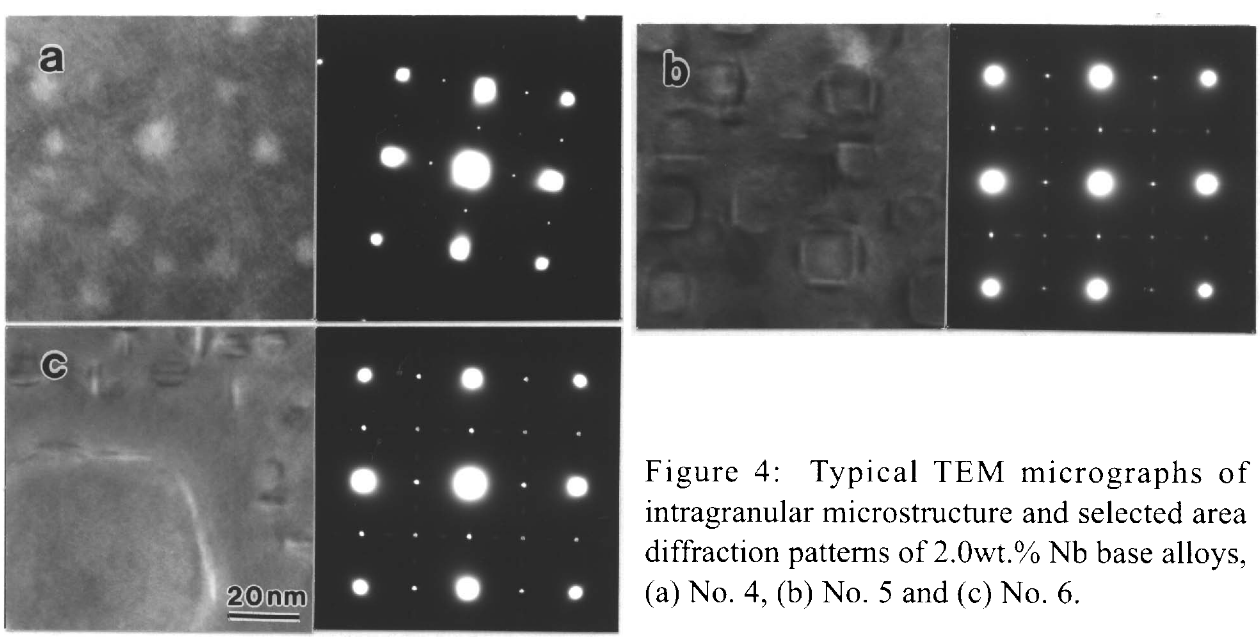

Figure 4: Typical TEM micrographs of intragranular microstructure and selected area diffraction patterns of 2.0wt.% Nb base alloys, (a) No. 4, (b) No. 5 and (c) No. 6.

TEM images and selected area diffraction patterns of the inside of grains of low Ti alloys are shown in Figure 6. In alloy No. 1 (a), γ′ phase of which size was about 20nm was observed. The precipitate of alloy No. 5 (b) was double cuboidal γ′-γ″ co-precipitate , while the precipitate of Alloy 706 (c) was γ′-γ″ overlaid co-precipitate, and the sizes of those precipitates were approximately 20nm and 13nm, respectively.

Figure 7 shows TEM images and selected area diffraction patterns of the inside of grains of alloys Nos. 3 and 6. A coarse γ′ phase was observed in alloy No. 3 which contains 1.0wt.% of Nb (a). The size of the precipitate was approximately 50nm and was much larger than those observed in alloys Nos. 1 and 5 and Alloy 706. In contrast to alloy No. 3, double cuboidal and overlaid γ′-γ″ co-precipitate simultaneously existed in 2.0wt.% Nb alloy (b).

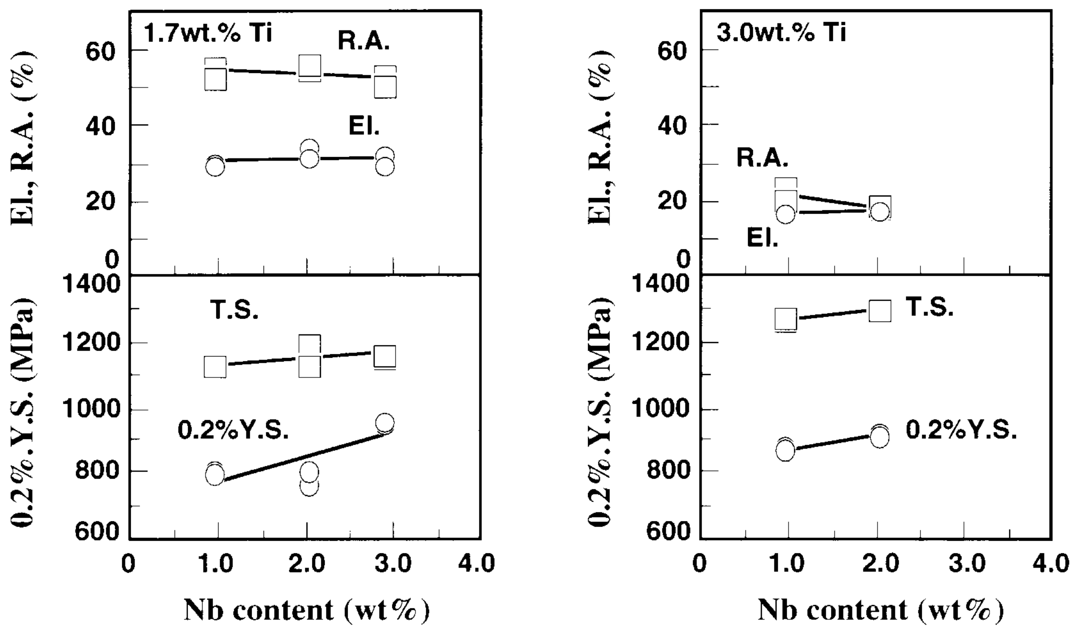

Figure 5: Variation of the tensile properties at room temperature with Nb content.

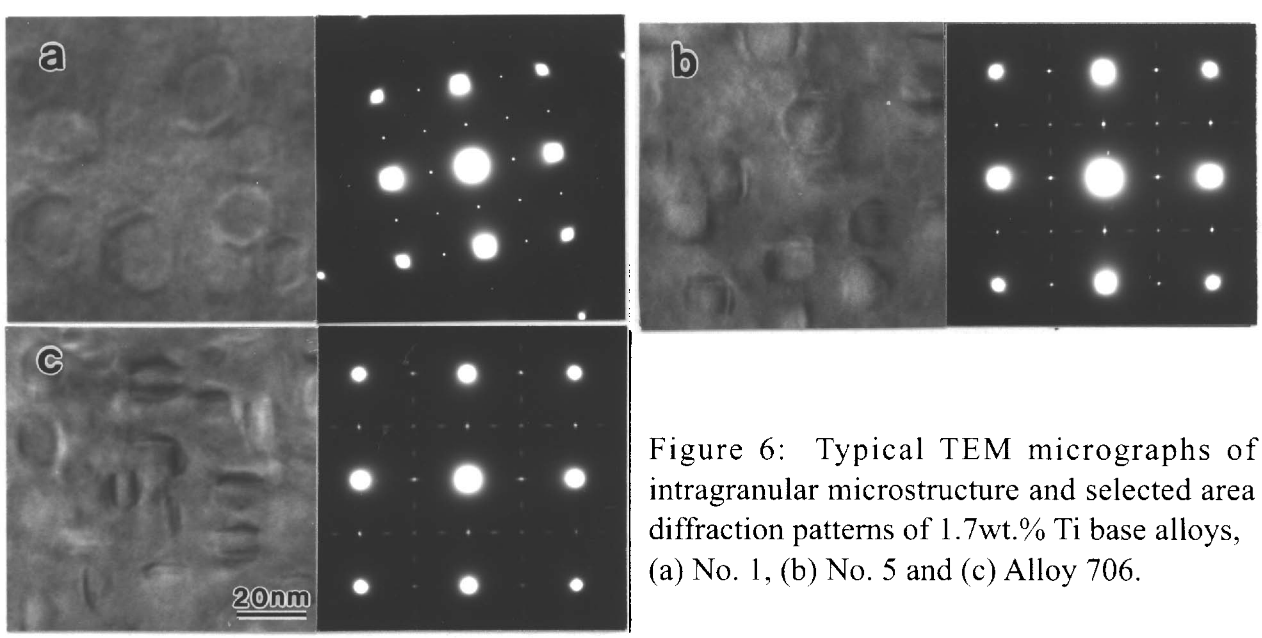

Figure 6: Typical TEM micrographs of intragranular microstructure and selected area diffraction patterns of 1.7wt.% Ti base alloys, (a) No. 1, (b) No. 5 and (c) Alloy 706.

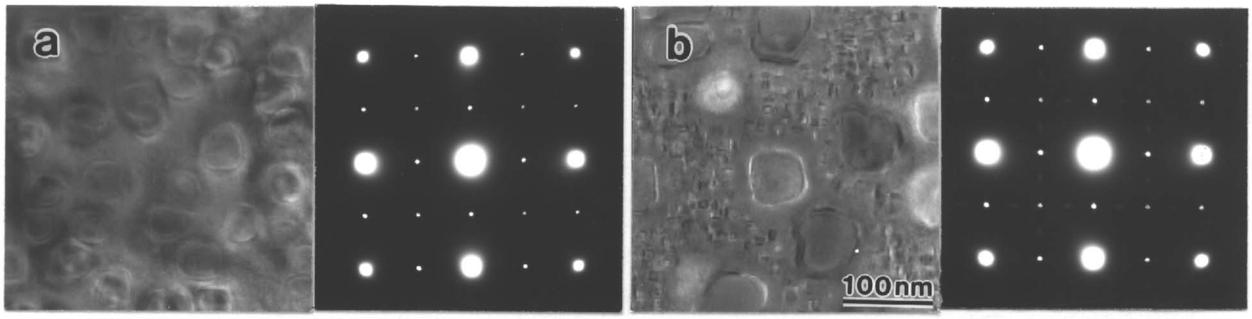

Figure 7: Typical TEM micrographs of intragranular microstructure and selected area diffraction patterns of 3.0% Titanium base alloys, (a) No. 3 and (b) No. 6.

Effect of Al Content

The variations of tensile properties of alloys Nos. 7 through 10 with Al content are shown in Figure 8. For both 2.1wt.% Nb base alloys and 2.6wt.% Nb base alloys, 0.2% yield strength decreased, whereas the remarkable change was not confirmed in tensile strength and the ductility, with increasing Al content. The influence of Al content on the tensile properties was much smaller than that of Ti content or Nb content. This difference is considered to reflect the difference in the lattice mismatch between hardening precipitate and matrix.

TEM images and selected area diffraction patterns of the inside of grains of alloys Nos. 7and 8 are shown in Figures 9 and 10. Regardless of Nb content, the intragranular precipitates had changed into γ' phase from double cuboidal γ'-γ' co-precipitates, with increasing Al content. In addition, the intragranular precipitates tend to become large with increasing Al content.

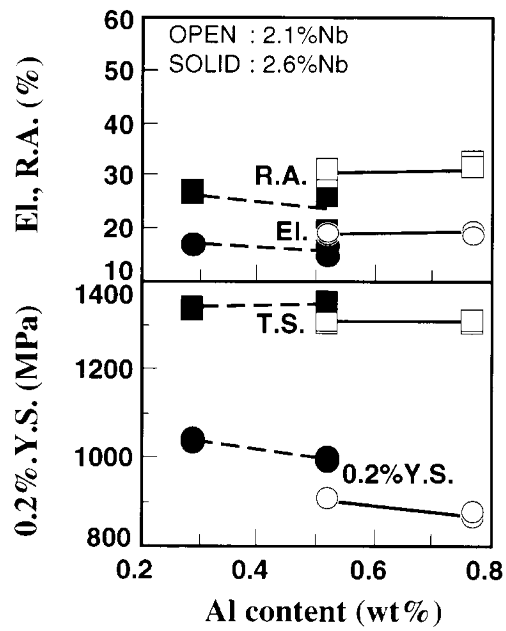

Figure 8: Variation of the tensile properties at room temperature with Al content.

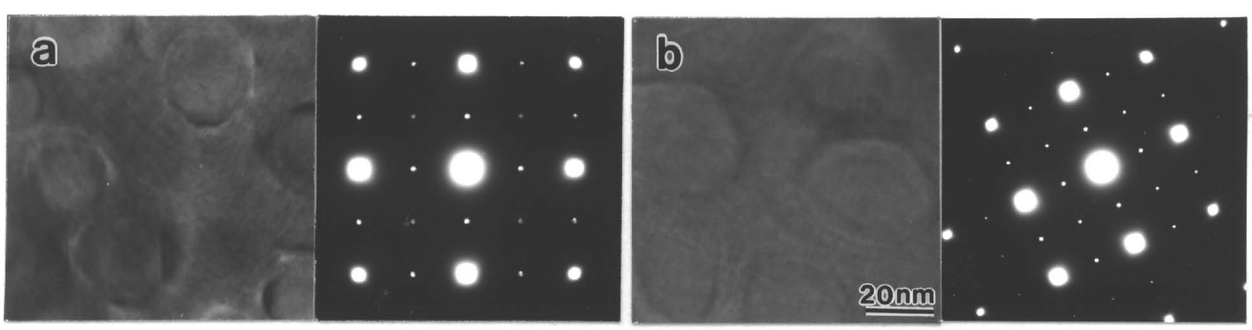

Figure 9: Typical TEM micrographs of intragranular microstructure and selected area diffraction patterns of 2.5wt.% Ti - 2.1wt.% Nb base alloys: (a) No. 7 and (b) No. 8.

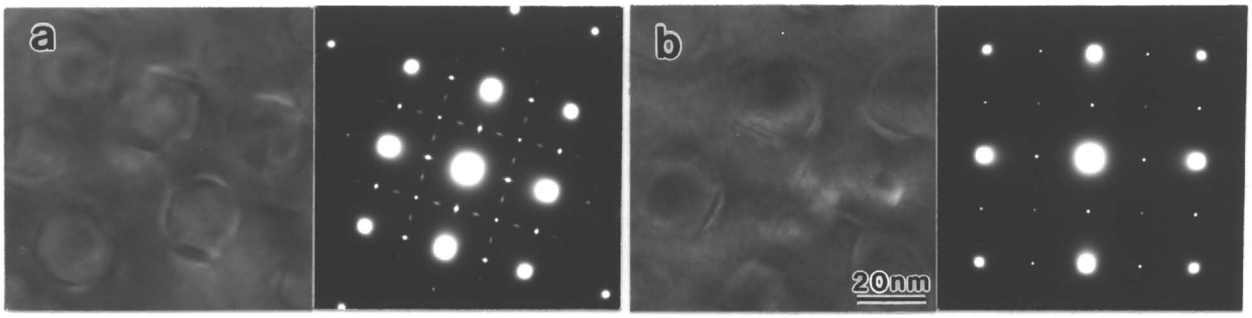

Figure 10: Typical TEM micrographs of intragranular microstructure and selected area diffraction patterns of 2.5wt.% Ti - 2.6wt.% Nb base alloys, (a) No. 9 (b) and No. 10.

<u>Compositional Range for γ'-γ'' co-precipitation</u>

From the above experimental results, the range of contents of Ti, Nb, and Al for γ'-γ'' co-precipitates to appear stably γ'-γ'' co-precipitate is shown in Figure 11. For γ'-γ'' co-precipitation, it is necessary for these three strengthening elements to simultaneously exist, and their contents are limited within the ranges, 1.5wt.% Ti or more, 1.5wt.% Nb or more, and between 0.3 and 0.5wt.% Al. When the contents of Al, Ti, and Nb are outside these ranges in Alloy 706 base matrix composition, effective higher strength cannot be expected. Accordingly, it is suggested that the content of each strengthening element be set near the upper limit within the range of stable precipitation to achieve higher strength effectively.

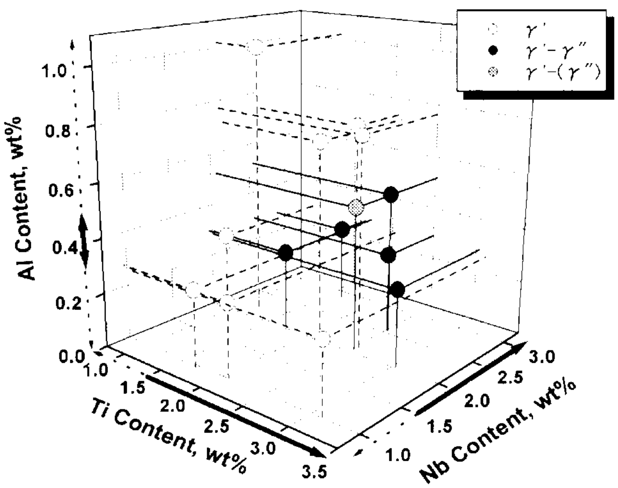

Figure 11: Range of composition for γ'-γ'' co-precipitation.

<u>Effect of Ta Content</u>

In addition to Ti, Nb, and Al, the effect of Ta as a precipitation strengthening element was investigated. The variation of tensile properties with Ta substitution ratio is shown in Figure 12. Both the strength and the ductility decreased with increasing Ta substitution ratio. Therefore, the addition of Ta does not contribute to the improvement of tensile properties.

TEM images and selected area diffraction patterns of the inside of grains of alloys Nos. 10 through 13 are shown in Figure 13. Although the main intragranular precipitates of alloy No. 10 are double cuboidal γ'-γ'' co-precipitate (b), only γ' phase existed inside grains when replacing Nb by Ta (a) and (c), and the size of γ'

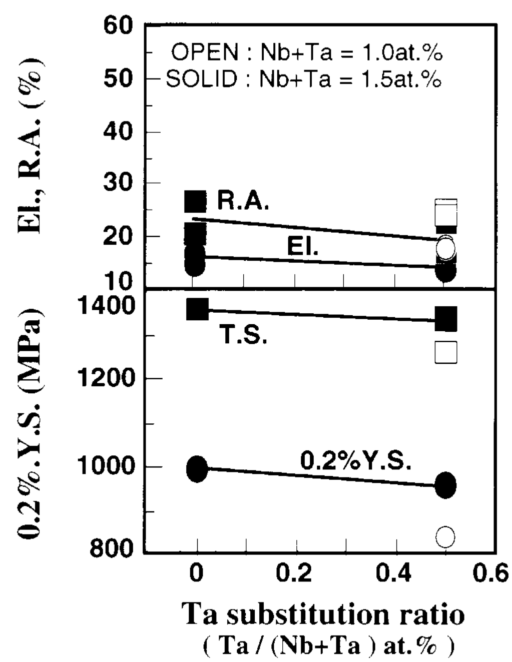

Figure 12: Variation of the tensile properties at room temperature with Ta substitution ratio.

phase tends to become large by Ta substitution. The reason why the addition of Ta is ineffective for higher strength is considered the appearance of the γ' phase which causes the decrease in strength.

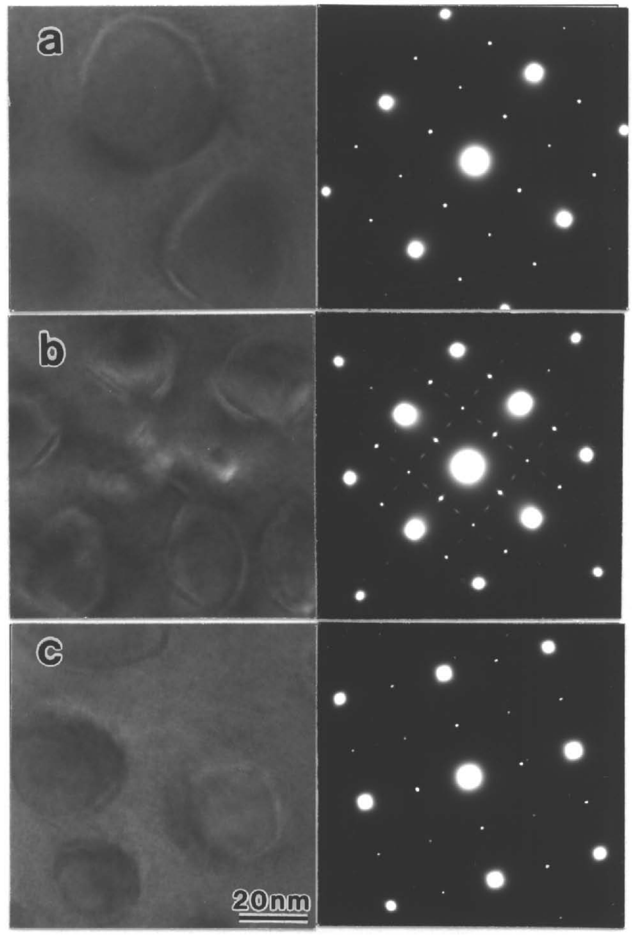

Figure 13: Effect of Ta substitution ratio on intragranular precipitation behavior,
alloys (a) No. 11, (b) No. 10 and (c) No. 12.

Results of Trial Manufacture

Based on the above mentioned results of fundamental research, we selected the best composition to optimize strength, ductility, and form of strengthening precipitates. The higher strength can be achieved by increasing Ti content and increasing Nb content. However, if both Ti content and Nb content are increased too much, TCP phase, such as Laves phase which will appear, degrades mechanical properties. On the other hand, Nb is more segregative element than Ti. So, Nb content should be minimized to reduce the segregation tendency. Therefore, the aimed chemical composition of main elements is set to low niobium and high titanium. Ni, Cr, and Al were fixed almost the same contents as Alloy 706. Then, the amount of Nb addition is decreased, the amount of Ti is increased and Ta is not added.

The large-size trial disk with the modified composition is shown in Figure 14. The trial disk was made from a double melted ingot (vacuum induction melting followed by electroslag remelting). The ingot size was 760mm in diameter by 2m in height, and the weight was approximately 7.2 ton. The diameter of the trial disk was 1680mm, the thickness was 245mm, and the weight was 4.4ton.

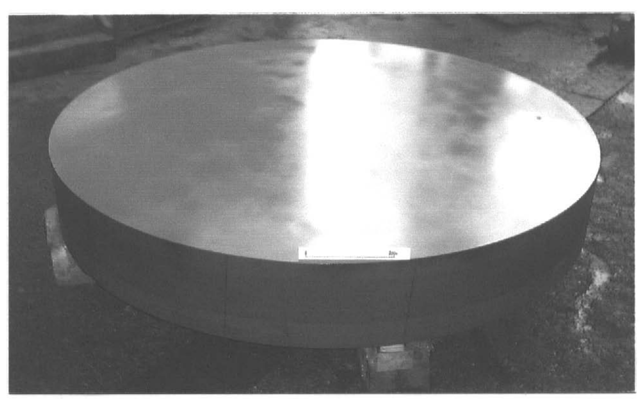

Figure 14: Appearance of traial disk.

As a result of the longitudinal wave radial test and the periphery near surface shear test, any defects such as cracks were not detected. The grain seize was about ASTM No. 3 in the whole of the trial disk. The macro-etching structure of the topside surface and longitudinal section revealed that no segregation existed. Chemical compositions at various portions in the disks were within the aimed range. As a result of TEM observation, γ'-γ'' co-precipitates were found dominantly inside grains in the whole of the disk, while the cellular precipitates identified as η phase were observed at the grain boundaries of the core portion. Mechanical testing confirmed that the strength of the trial disk was comparable to specification of Alloy 718 (AMS5653). Moreover, the ductility and the toughness greatly exceeded the specification of Alloy 718.

Conclusions

In order to modify the chemical composition of Alloy 706, the effects of precipitation strengthening elements on tensile properties and precipitation behavior were investigated in detail. Furthermore, compositional modification was conducted and the large-size trial disk was manufactured. Conclusions are summarized as follows.

(1) The strength increased and the ductility decreased with increasing the contents of Ti and Nb. The 0.2% yield strength decreased, although the tensile strength and the ductility did not change, with increasing Al content. Both the strength and the ductility decreased, with increasing Ta substitution ratio (increasing Ta content and decreasing Nb content)

(2) The intragranular precipitation behavior was greatly affected by the contents of Ti, Nb, and Al. In order for γ'-γ'' co-precipitate to appear, these three strengthening elements are needed to simultaneously exist. Their contents are limited within the ranges, 1.5wt.% Ti or more, 1.5wt.% Nb or more, and between 0.3 and 0.5wt.% Al.

(3) The large-size trial disk with modified composition had good mechanical properties without any segregation. The characteristics regarding strength, ductility and toughness were comparable to those of Alloy 718. The intragranular precipitates were double cuboidal γ'-γ'' co-precipitate and the results obtained agreed with those expected.

References

1. P.W.Schilke, J.J.Pepe and R.C.Schwant, "Alloy 706 Metallurgy and Turbine Wheel Application," Superalloys 718,625,706 and Various Derivatives, ed. E.A.Loria, (Warrendale, PA:TMS, 1994), 1-12.
2. A.D.Helms, C.B.Adasczik and L.A.Jackman, "Extending the Size Limits of Cast/Wrought Superalloy Ingots," Superalloys 1996, ed. R.D.Kissinger et al., (Warrendale, PA:TMS, 1996), 427-433.
3. R.C. Schwant, "Large 718 Forgings for Land Base Turbines," Superalloys 718,625,706 and Various Derivatives, ed. E.A.Loria, (Warrendale, PA:TMS, 1997), 141-152.
4. E.E.Brown and D.R.Muzyka, "Nickel-Iron Alloys," Superalloys II, ed. C.T.Sims, N.S.Stoloff, and W.C.Hagel, (New York, John Wiley & Sons, 1987), 165-188.
5. T. Shibata, Y. Shudo and Y. Yoshino, "Effects of Aluminum, Titanium and Niobium on the Time - Temperature - Precipitation Behavior of Alloy 706," Superalloys 1996, ed. R.D.Kissinger et al., (Warrendale, PA:TMS, 1996), 153-162.
6. T. Shibata et al., "Effect of Stabilizing Treatment on Precipitation Behavior of Alloy 706," ibid., 627-636
7. Scott A. Loewenkamp and John F. Radavich, "Microstructure vand Properties of Ni-Fe Base Ta-718," Superalloys 1988, ed. D.N.Duhl et.al., (Warrendale, PA:TMS, 1988), 53-62.
8. Andrea R. Braun and John F. Radavich, "A Microstructural and Mechanical Properties Comparison of P/M 718 and P/M TA 718," Superalloy 718-Metallurgy and Applications, ed. E.A. Loria, (Warrendale, PA:TMS, 1989), 623-629.
9. T.Takahashi et al., "Effects of Grain Boundary Precipitation on Creep Rupture Properties of Alloy 706 and 718 Turbine Disk Forgings," Superalloys 718,625,706 and Various Derivatives, ed. E.A.Loria, (Warrendale, PA:TMS, 1994), 557-565.
10. X. Xie et al., "Investigation on High Stability and Creep Resistant Modified Inconel 718 with Combined Precipitation of γ'' and γ'," ibid., 711-720.
11. E. Guo, F. Xu and E.A. Lolia., "Further Studies on Thermal Stability of Modified 718 Alloys," ibid., 721-734.
12. E.Andrieu, R.Cozar, and A. Pineau, "Effect of Environment and Microstructure on The High Temperature Behavior of Alloy 718," Superalloy 718-Metallurgy and Applications, ed. E.A. Loria, (Warrendale, PA:TMS, 1989), 241-256.